

NATIONAL RADIO ASTRONOMY OBSERVATORY
GREEN BANK, WEST VIRGINIA 24944

ELECTRONICS DIVISION INTERNAL REPORT No. 181

CRYOGENICALLY-COOLED C-BAND PIN DIODE SWITCH

GEORGE H. BEHRENS, JR.

OCTOBER 1977

NUMBER OF COPIES: 150

CRYOGENICALLY-COOLED C-BAND PIN DIODE SWITCH

George H. Behrens, Jr.

Introduction:

This report deals with a cryogenically-cooled, C-band, PIN diode switch developed for radio astronomy applications. The various switching modes available, principles of operation, operating characteristics and construction details are discussed.

The switch was developed to satisfy the Dicke switching requirements for a new low noise, dual band (25 cm and 6 cm), dual channel, cryogenic radiometer under construction at NRAO. The design goal was to achieve a switch with minimum loss, VSWR and noise contribution which could operate at cryogenic temperatures over the frequency band from 4.5 - 5.1 GHz and provide the necessary Dicke switching functions as dictated by the various types of astronomical observations.

The Dicke Radiometer: [1]

In radio astronomy the signal levels received are of such low levels that receiver gain instabilities can seriously limit the effective sensitivity of the radiometer. This effect can be minimized by using the Dicke radiometer as shown in Figure 1A. The receiver input is continuously switched between the antenna feed horn and a comparison noise source at a frequency high enough so that the gain has no time to change during one cycle.

The detected output V_0 of the Dicke radiometer is proportional to the difference between the antenna noise temperature T_A and the noise temperature of the comparison noise source T_C :

$$V_0 = K (T_A - T_C), \quad (1)$$

[1] J. D. Kraus, Radio Astronomy. New York: McGraw-Hill, 1966.

and the minimum detectable signal is given by the following expression if

$$T_A = T_C:$$

$$\Delta T_{\min} = 2 T_R \sqrt{\frac{1}{\beta \tau}} \quad (2)$$

where:

T_R = receiver noise temperature, °K.

β = predetection bandwidth, Hz.

τ = integration time, sec.

In practice the comparison noise source is usually either a microwave termination held at a fixed physical temperature or another antenna feed horn. When a cryogenic receiver is used, the termination is usually held at the operating temperature of the refrigerator (e.g., 20°K). Antenna temperatures are usually around 20°K also, so $T_A \approx T_C$. If there is a significant unbalance between T_A and T_C , noise can be injected via a directional coupler, into the colder channel to balance the system or the receiver gain can be reduced during the higher temperature half of the switch cycle.

When a feed horn is used as the comparison noise source, it is usually identical to the signal feed horn. Both horns are then offset laterally by equal amounts from the focal point of the reflector insuring equal noise temperatures for both feeds. This method has the advantage that fluctuations in antenna temperature caused by atmospheric conditions are effectively cancelled since the beams of both feeds see essentially the same area of the atmosphere because their beams are usually only on the order of 2-3 half power beam widths apart. However, when observations are made of extended sources, it is advantageous to use the switch load mode of operation; otherwise, both

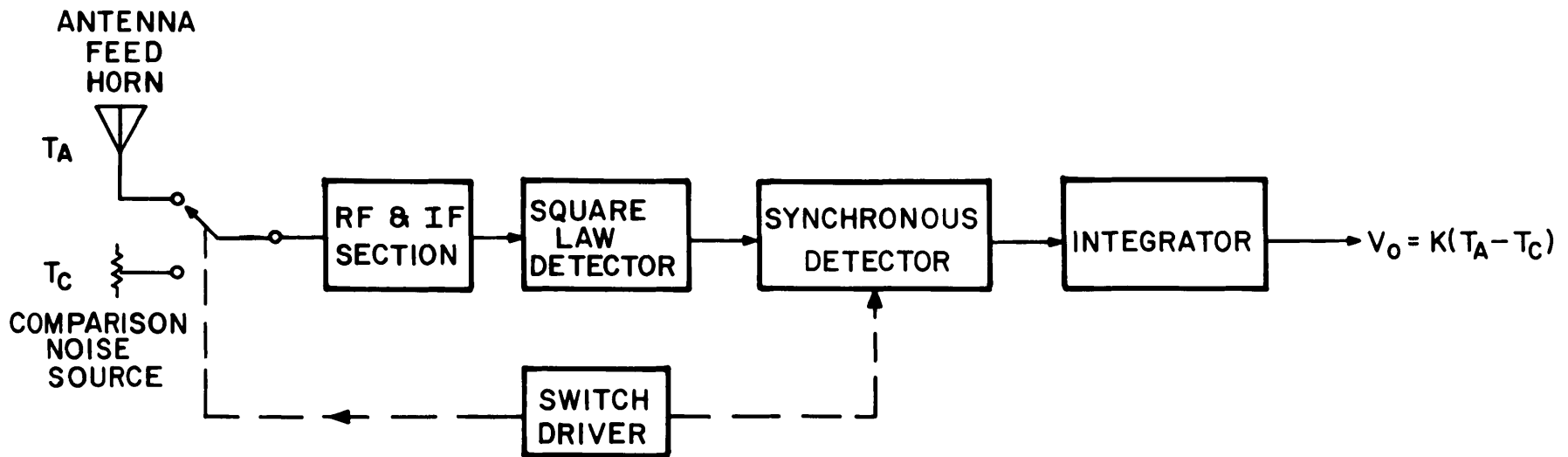


FIG. 1A SINGLE CHANNEL DICKE RADIOMETER

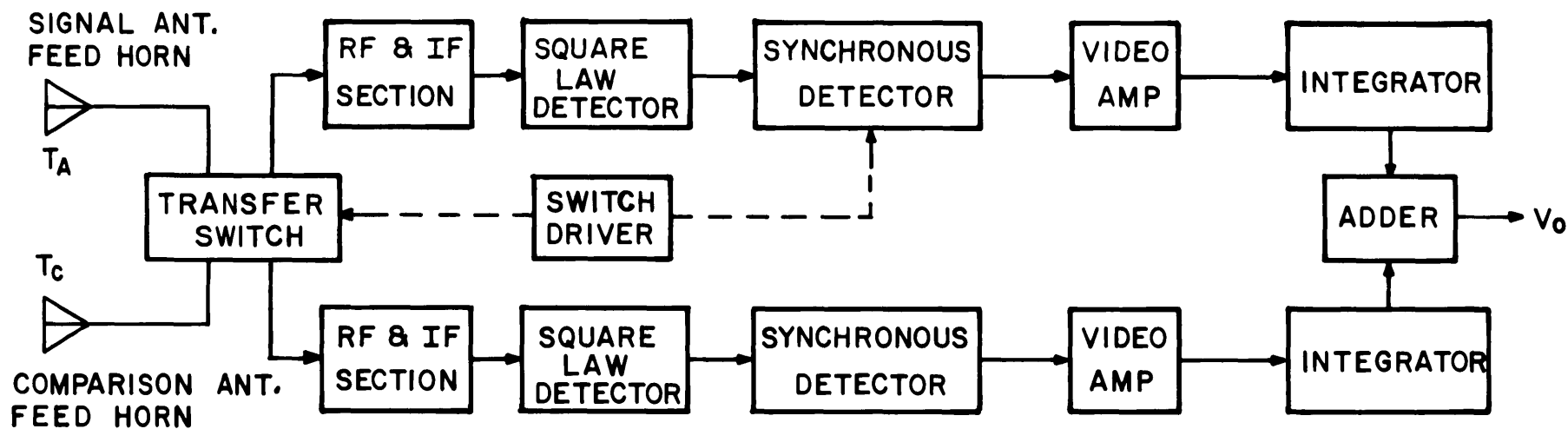


FIG.1B DUAL CHANNEL DICKE RECEIVER USING THE SWITCH BEAM CONFIGURATION

beams will be on source and the output will be distorted. It is therefore desirable in the design of a radiometer to incorporate a means to provide both a beam switching mode and a load switching mode.

Dual Channel Operation:

In the single channel Dicke radiometer the signal power is observed only half of the time. However, by switching the signal feed horn between two receivers and adding their outputs as shown in Figure 1B, the efficiency of the radiometer is increased. It can be shown that the minimum detectable signal noise temperature of a dual channel Dicke radiometer is reduced by a factor of $\sqrt{2}$ over a single channel radiometer. In order to achieve the necessary switch action for a dual channel Dicke receiver using the beam switching mode a transfer switch is required.

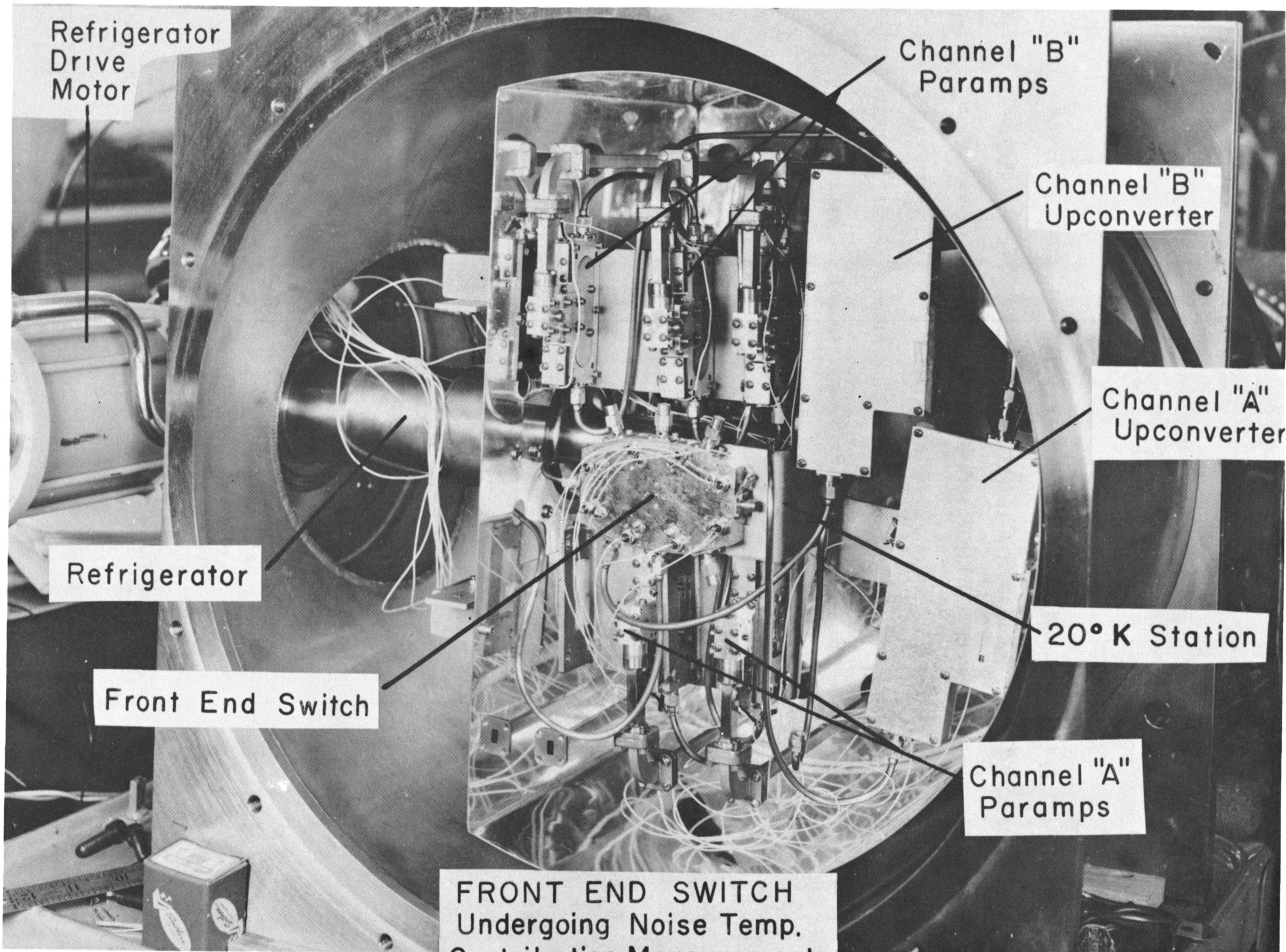
Dicke Switch Design Considerations:

One of the major disadvantages of a Dicke radiometer is the degradation of system noise temperature due to the noise temperature of the Dicke switch. The amount of noise added to the system by the loss mechanism of the switch is:

$$\Delta T_S = (T_P + T_R) (L - 1) \quad (3)$$

where:

- ΔT_S = noise added to system due to switch.
- T_P = physical temperature of switch.
- L = loss of switch.
- T_R = receiver input noise temperature.



Refrigerator
Drive
Motor

Channel "B"
Paramps

Channel "B"
Upconverter

Channel "A"
Upconverter

Refrigerator

20° K Station

Front End Switch

Channel "A"
Paramps

FRONT END SWITCH
Undergoing Noise Temp.
Contribution Measurements

FIG. 2

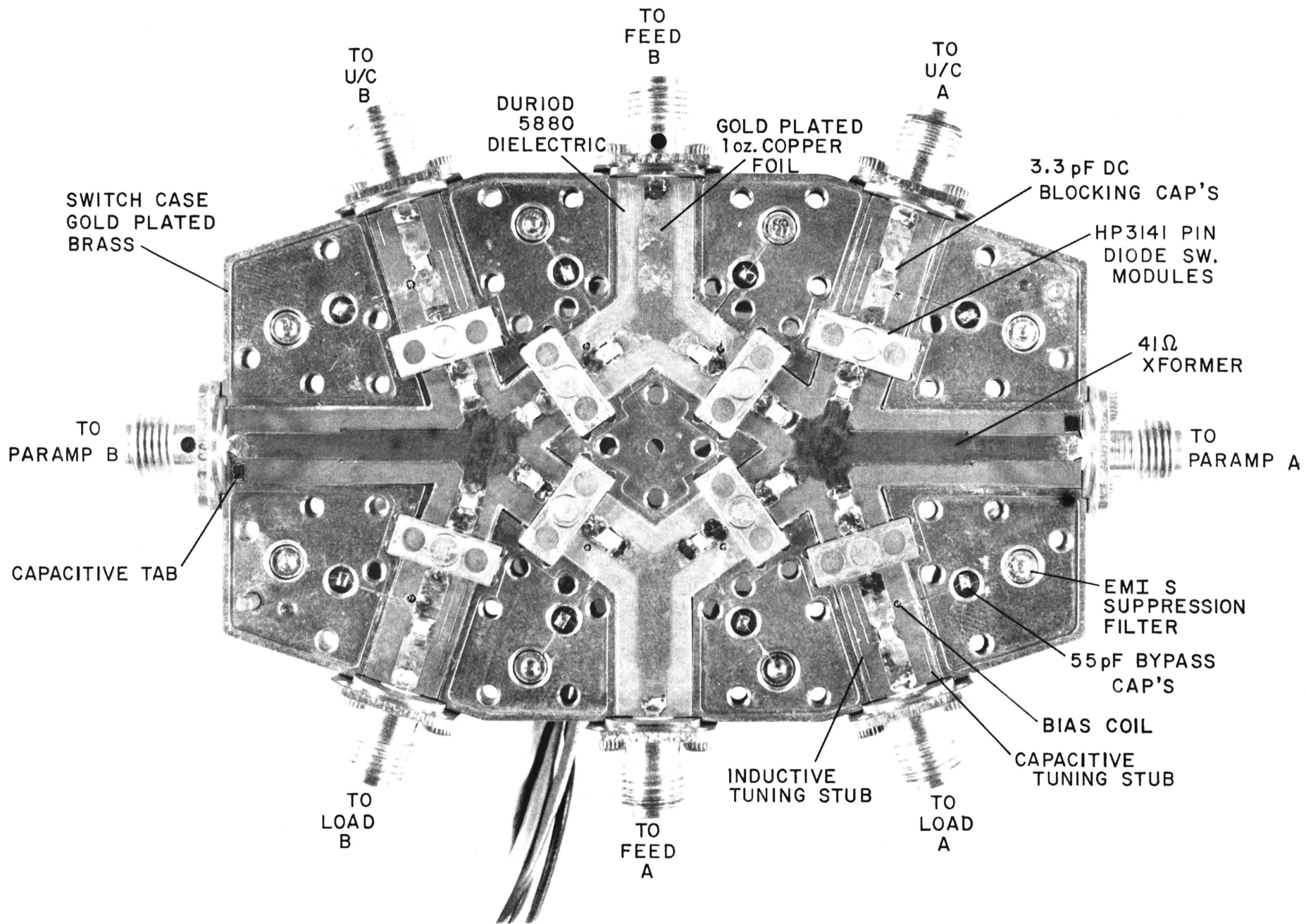


FIG. 3 FRONT END SWITCH FOR 25cm / 6cm RECEIVER

Therefore, to minimize ΔT_s , both the physical temperature T_p and the loss L of the switch should be kept to a minimum. In the 25/6 cm radiometer, to minimize T_p the Dicke switch is mounted directly to the 20°K station of the refrigerator as shown in Figure 2.

In planning the 25/6 cm radiometer, it was decided that a dual channel Dicke radiometer be implemented. It was also decided that the Dicke switch, besides providing the transfer switching function needed for dual channel operation, should also incorporate a means to permit either load switching or beam switching for either channel. Further, it was decided that the switch be used to connect the L-band upconverters to the parametric amplifiers during 25 cm operation. Dicke switching is not needed during 25 cm operation because only line observations are performed and they are relatively unaffected by gain instabilities.

TABLE 1

RF Paths thru Switch for Various Switching Modes

No.	Switching Mode	Connections Made During Switching Cycle	
		First Half Switching Cycle	Second Half Switching Cycle
I.	Both Channels Load Switching	2 → A 5 → B	1 → A 3 → B
II.	Both Channels Beam Switching	2 → A 5 → B	5 → A 2 → B
III.	Channel A Beam Switching Channel B Load Switching	2 → A 5 → B	5 → A 3 → B
IV.	Channel A Load Switching Channel B Beam Switching	2 → A 5 → B	1 → A 2 → B
V.	Both Channels Locked to Upconverters	6 → A 4 → B	No switching.

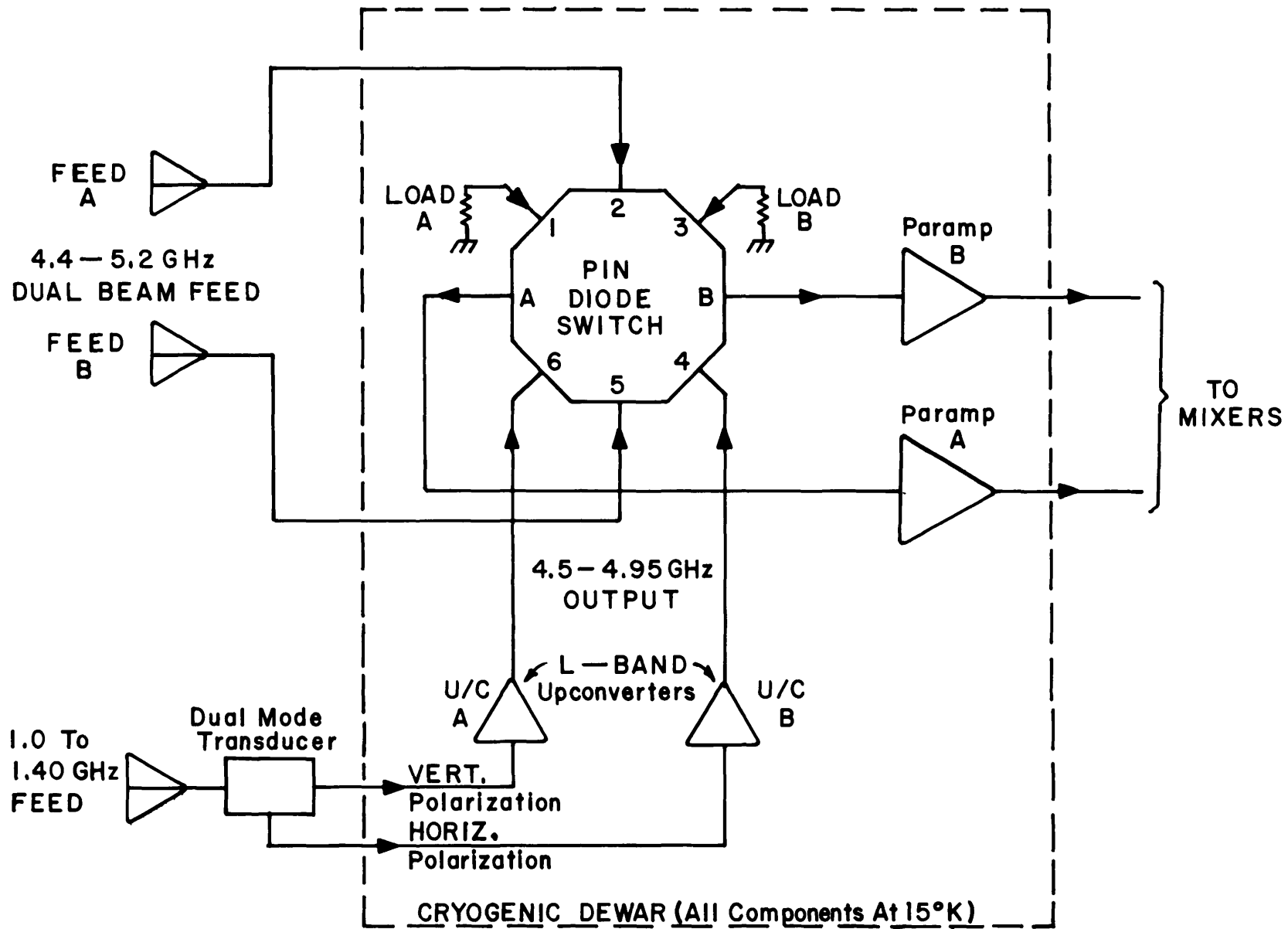


FIG.4 Block Diagram Of The Front End Section Of The 25/6cm Cryogenic Radiometer

The switch is a combination transfer switch and two SP4T switches which provides various switching modes best described by referring to Table 1 and Figure 4. As shown in Table 1 there are five different switching modes available. The table shows the connections for the various modes for each half of the switching cycle, e.g., in mode I (both channels load switching), Feed A is connected to Paramp A and Feed B is connected to Paramp B during the first half switching cycle. During the second half of the switching cycle, loads A and B are connected to Paramps A and B, respectively.

Principles of Operation:

Referring to Figure 5, the operation of the switch in the Beam Switch Mode can be explained as follows. Assume RF energy is propagating from Feeds A and B towards junctions J1 and J2, respectively, and diodes D1 thru D8 are biased as shown during the first half switching cycle. Next consider how the energy from Feed A divides at J1 due to the impedance conditions at J1 as seen looking towards JA and JB. Since D3 is forward biased, its low impedance (see Figure 6A) is transformed to a high impedance at J1 by the quarter wavelength 50 ohm transmission line according to the usual quarter wave transformer equation:

$$Z_{IN} = Z_0^2 / Z_d \quad (4)$$

where:

Z_0 = characteristic impedance of line.

Z_d = forward biased diode impedance.

However, the impedance at J1, as seen looking towards JA, is close to 50 ohms since D2 is reverse biased and presents little affect on the line since its impedance is high (see Figure 6B). Also, diodes D1, D7 and D8 are

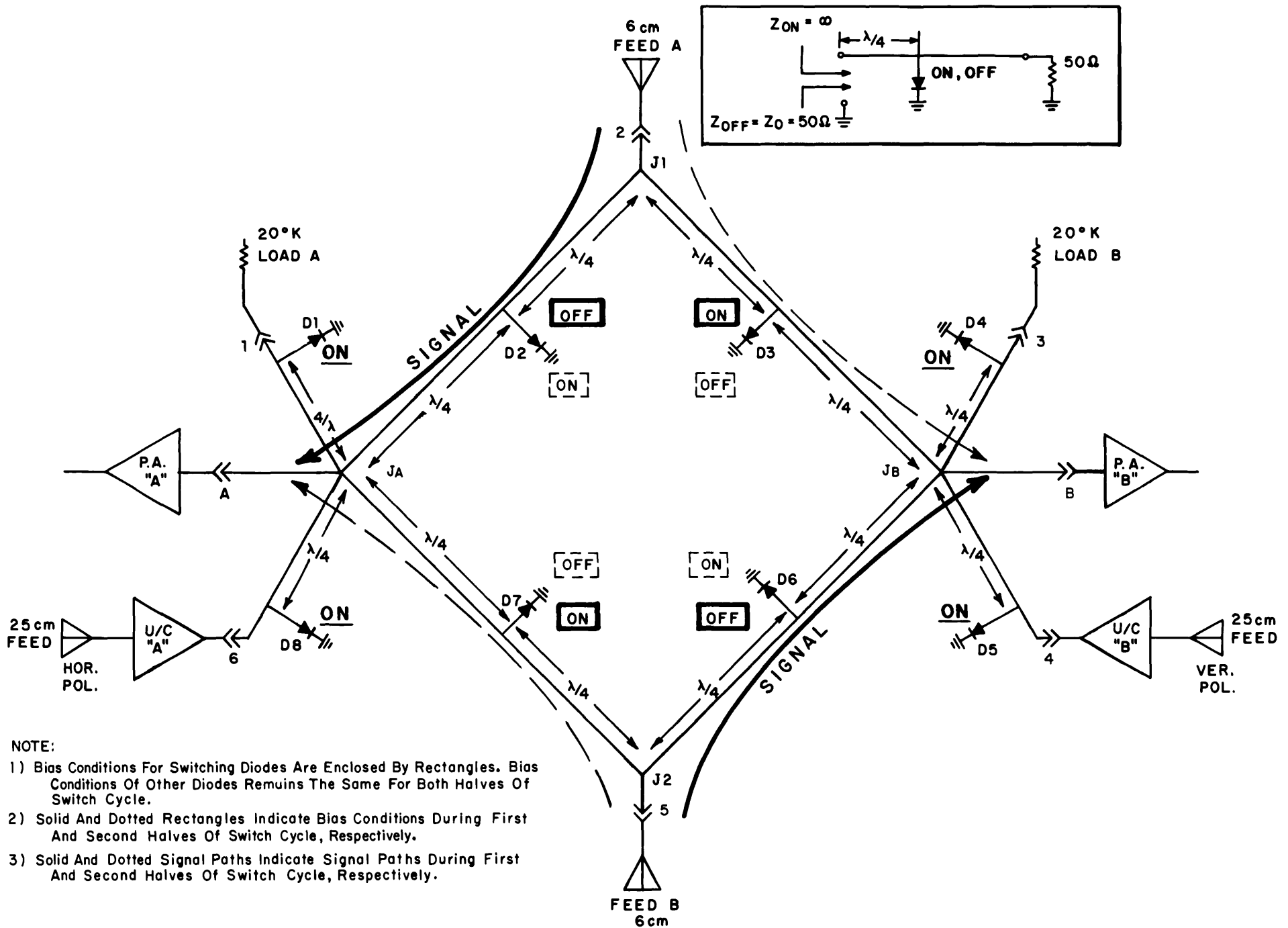
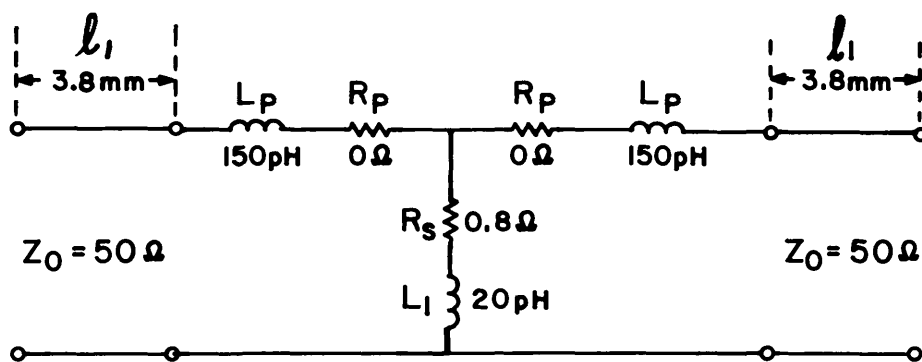
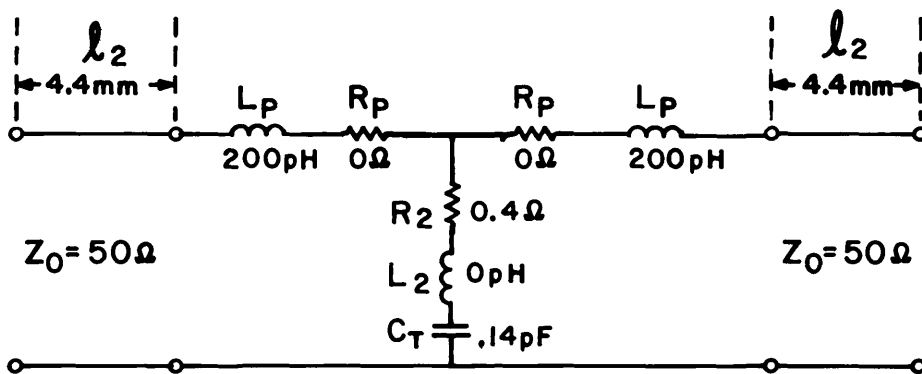


FIG. 5 Simplified Schematic Of Front End Switch Operating In The Beam Switching Mode.



(a) Forward Bias



(b) Reverse Bias

FIG. 6 Room Temperature Equivalent Circuit Of
HP 5082-3141 PIN Diode

forward biased causing the impedance looking into each of these arms from JA to be high. Therefore, all the energy entering J1 from Feed A is directed to Paramp P.A. "A" except for the relatively small losses absorbed in the high impedance arms of junctions JA and J1.

The energy arriving at J2 from Feed B can similarly be analyzed to show that it is directed to P.A. "B". During the next half switching cycle the bias conditions of D2, D3, D6 and D7 are reversed causing the RF energy to be directed from Feed A and B to P.A. "B" and "A", respectively. The operation of the switch in the other modes can be explained similarly by referring to Table 2 which gives the bias conditions for the various switching modes.

TABLE 2

Bias Condition of Diodes for Different Switching Modes

Mode		I		II		III		IV		V	
Half of sw. cycle		1st	2nd								
DIODES	D1 ...	FWD	REV	<i>Fwd</i>	<i>Fwd</i>	<i>Fwd</i>	<i>Fwd</i>	FWD	REV	<i>Fwd</i>	<i>Fwd</i>
	D2 ...	REV	FWD	REV	FWD	REV	FWD	REV	FWD	<i>Fwd</i>	<i>Fwd</i>
	D3 ...	<i>Fwd</i>	<i>Fwd</i>	FWD	REV	<i>Fwd</i>	<i>Fwd</i>	FWD	REV	<i>Fwd</i>	<i>Fwd</i>
	D4 ...	FWD	REV	<i>Fwd</i>	<i>Fwd</i>	FWD	REV	<i>Fwd</i>	<i>Fwd</i>	<i>Fwd</i>	<i>Fwd</i>
	D5 ...	<i>Fwd</i>									
	D6 ...	REV	FWD	REV	FWD	REV	FWD	REV	FWD	<i>Fwd</i>	<i>Fwd</i>
	D7 ...	<i>Fwd</i>	<i>Fwd</i>	FWD	REV	FWD	REV	<i>Fwd</i>	<i>Fwd</i>	<i>Fwd</i>	<i>Fwd</i>
	D8 ...	<i>Fwd</i>									

Capital letters are used to indicate bias condition of diodes switching in that particular mode. Bias conditions of diodes in a fixed bias state are italicized.

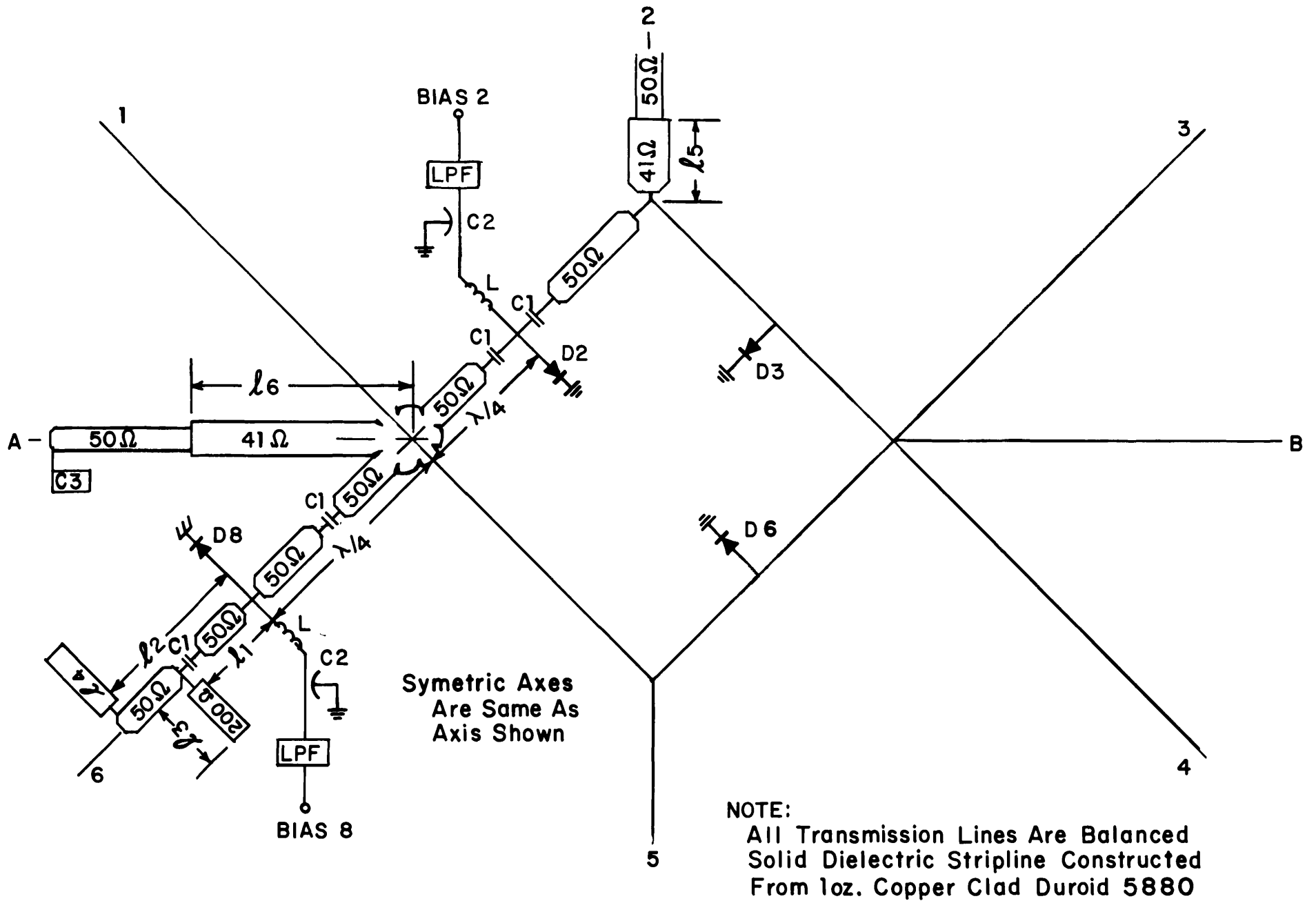


FIG. 7 Diagramatic Layout Of Switch

The complete schematic of the switch is shown in Figure 7. Table 4 gives the values of the various components and the manufacturers' part number.

The 50 ohm transmission line system used is balanced stripline constructed from photographically etched, copper clad, .0625" thick, teflon/fiberglass. The ground planes are formed by the gold plated brass case (see Figure 3). Channels 0.300" wide by .062" deep were milled in the switch case to accommodate the stripline material. This type of construction was used to maximize isolation between the various arms and achieve good mechanical stability. The ground plane spacing is 0.125" and the gold plated copper (1 oz) center conductor is 0.100" wide for $Z_0 = 50$ ohms. A small lip was left along the edge of all channels to improve mating surfaces and minimize radiation leakage.

The switching diodes, HP 5082-3141, are silicon PIN diodes incased in a 50 ohm hermetic package which permits a continuous transition in the 50 stripline circuit. This stripline package concept, according to Hewlett-Packard, overcomes the limitations in insertion loss, isolation and bandwidth that are imposed by the package parasitics of other discrete devices.

The photograph in Figure 3 shows the physical layout of the various components.

TABLE 4

Component Data

<u>Components</u>	<u>Value</u>	<u>Function</u>	<u>Manufacturer's P/N</u>
C ₁	3.3 pF	Blocking capacitor	ATC-100A-3R3-P-50
C ₂	56 pF	Bypass capacitor	ATC-100A-560-K-P-50
C ₃	0.05" x .075"	Capacitive tap	---
L	---	Bias Injection coil	Pionics 9 1/2 T-47
LPF	---	EMI suppression filter	Erie #1250-003
D1-D8	---	PIN diode	HP 5082-3141
Stripline material	$\epsilon = 2.23$	---	R/T Duroid 5880
l ₁	$Z_0 = 50 \Omega$ $l = .27"$	Transmission line	---
l ₂	$Z_0 = 50 \Omega$ $l = .573$	Transmission line	---
l ₃	$Z_0 = 200 \Omega$ $l = .700"$	Inductive tuning stub	---
l ₄	$Z_0 = 200 \Omega$ $l = 0.195$	Capacitive tuning stub	---
l ₅	$Z_0 = 41 \Omega$ $l = .36"$	Impedance transformer	---
l ₆	$Z_0 = 41 \Omega$ $l = .55"$	Impedance transformer	---

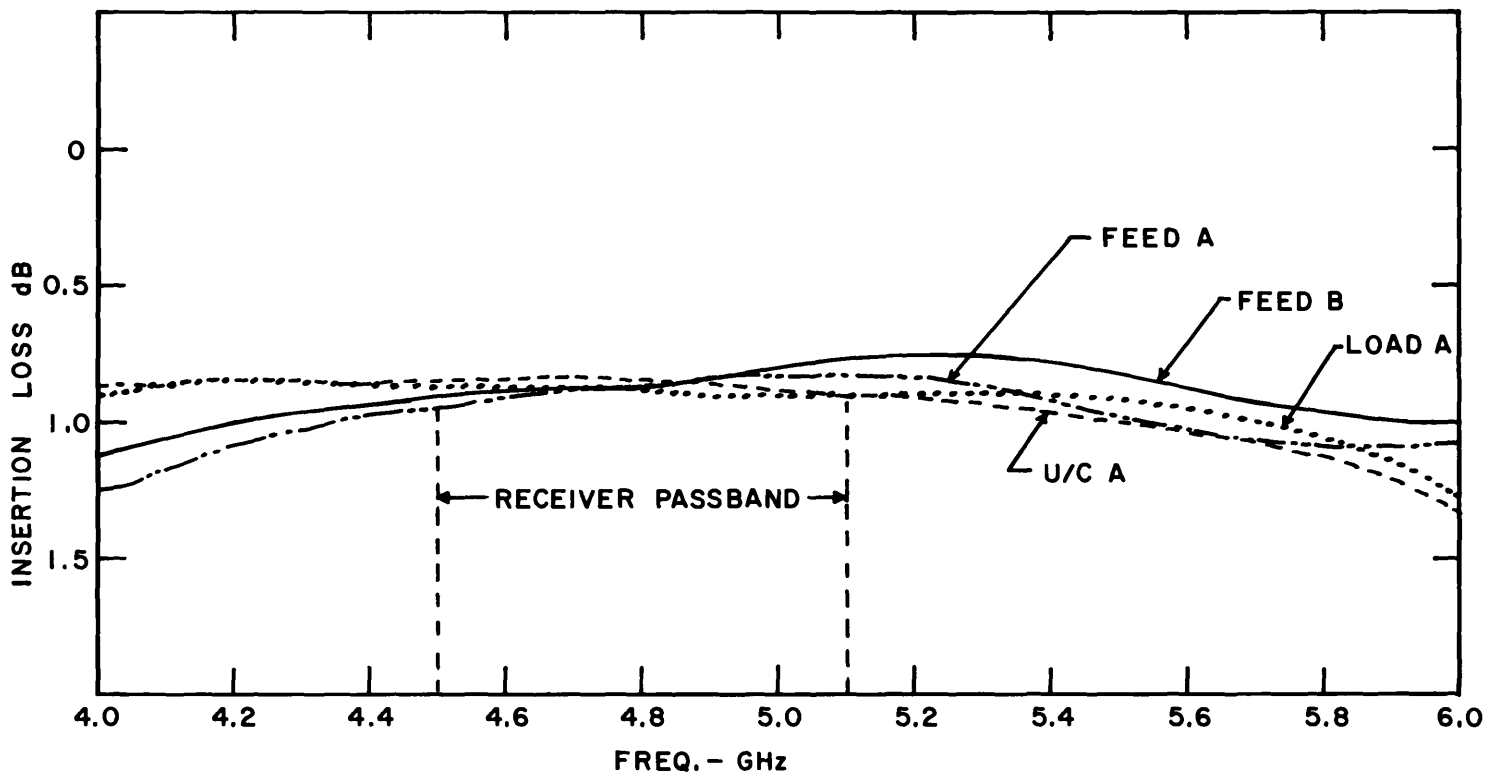


FIG. 8 INSERTION LOSS PARAMP "A" → INDIVIDUAL PORTS T=300°K, I=20mA/DIODE

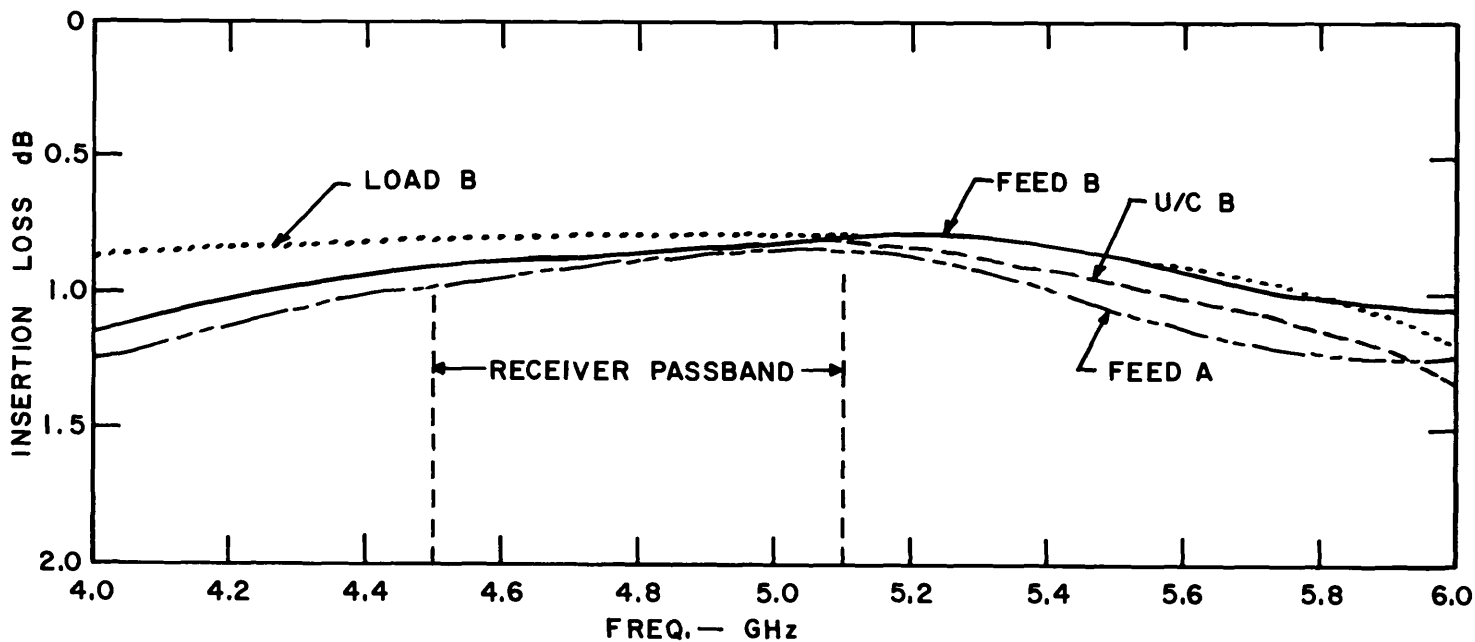


FIG. 9 INSERTION LOSS PARAMP "B" INDIVIDUAL PORTS T=300°K, I=20mA/DIODE

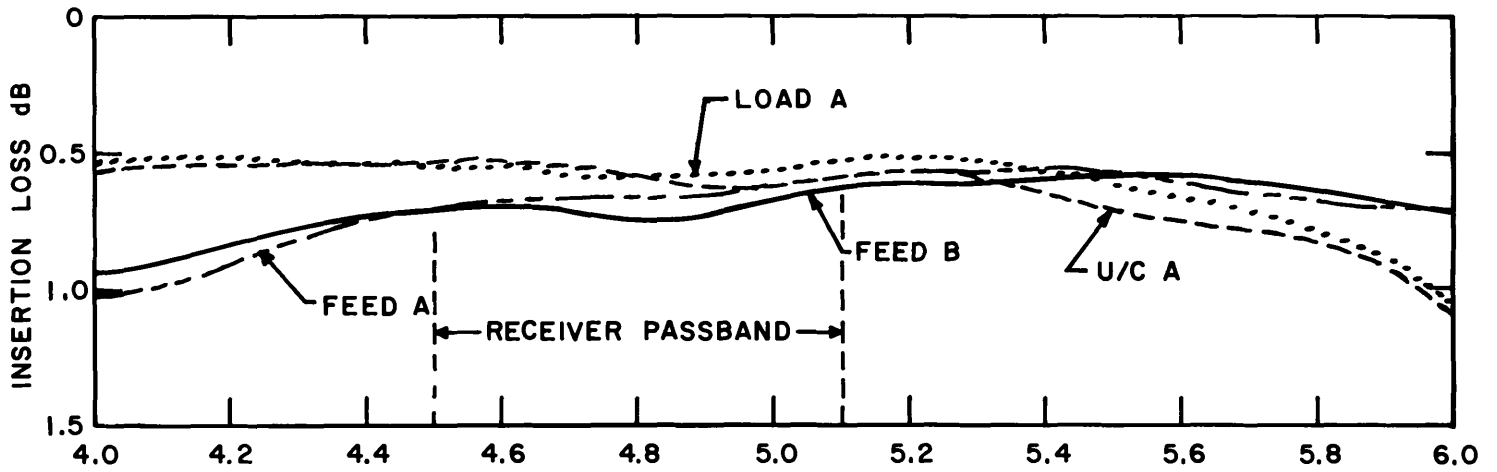


FIG. 10 INSERTION LOSS PARAMP "A" INDIVIDUAL PORTS

T=18°K, I=150mA/DIODE

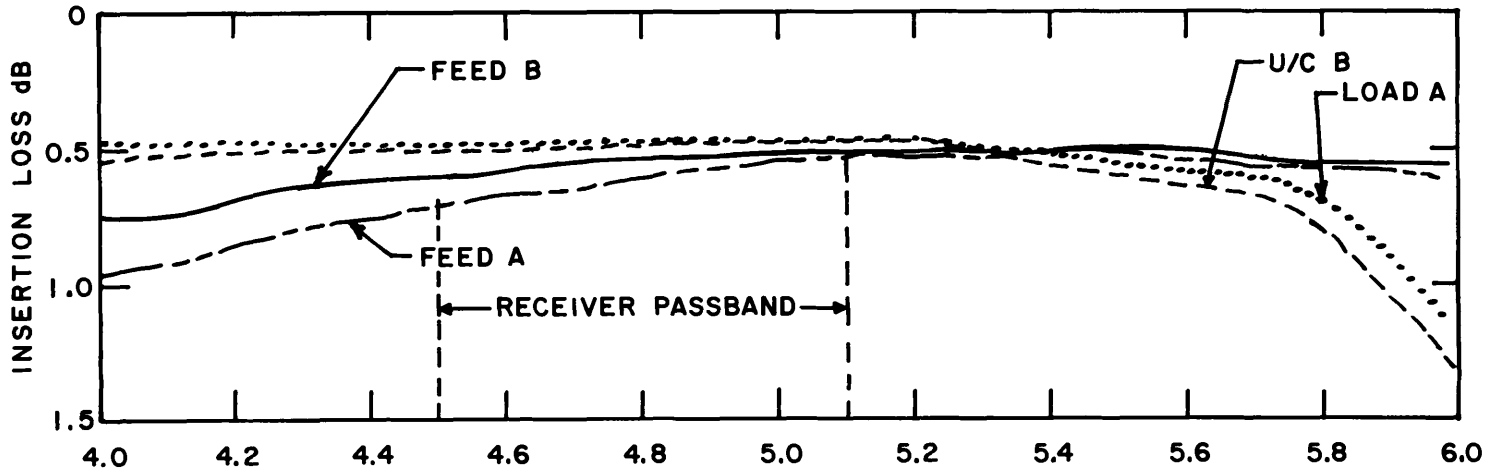


FIG. 11 INSERTION LOSS PARAMP "B" INDIVIDUAL PORTS

T=18°K, I=150mA/DIODE

TABLE 5

Measured Noise Contribution due to Dicke Switch

	Feed A °K	Feed B °K
<u>Channel A</u>		
Continuum, 4.245-5.040	12.8	14.9
4.6 GHz, 3% bandwidth	10.2	13.3
4.75 GHz, 3% bandwidth	15.2	16.9
4.870 GHz, 3% bandwidth	11.8	13.0
4.920 GHz, 3% bandwidth	13.0	10.0
Average	12.55	13.5
<u>Channel B</u>		
4.245 - 5.040	17.4	14.3
4.6 GHz, 3% bandwidth	13.7	9.6
4.75 GHz, 3% bandwidth	18.9	16.76
4.870 GHz, 3% bandwidth	17.8	12.2
4.920 GHz, 3% bandwidth	17.5	14.7
Average	17.0	13.3

A summary of the measured switch characteristics are given in Tables 6 and 7.

TABLE 6

Switch Characteristics over 4.4 - 5.1 GHz Band

	Channel A	Channel B
Maximum insertion loss (dB)	0.75	0.75
Maximum noise contribution (°K)	16.9	18.9
Average noise contribution (°K)	13.0	15.2
Maximum VSWR	1.5:1	1.5:1
Minimum isolation (dB)	30	30

TABLE 7

Switch Characteristics over 4.0 - 6.0 GHz Band

	Channel A	Channel B
Maximum insertion loss (dB)	1.1	2.0
Noise contribution	Not measured	Not measured
Maximum VSWR	< 2.0:1	< 2.0:1
Minimum isolation (dB)	30	30

Performance:

Measurements were made to determine switch insertion loss, isolation, reflection coefficient and noise contribution at both 18°K and room temperature conditions. Results of the insertion loss measurements are shown in Figures 8 thru 11. At 18°K the switch has a maximum loss of 0.75 dB over the operating band of the receiver. Isolation measurements, made in the 4.0-6.0 GHz band, revealed greater than 30 dB isolation between ports. VSWR measurements indicate a maximum VSWR of 1.5:1 in the pass band of the receiver and a maximum of 2.0:1 from 4.0 - 6.0 GHz. Noise contribution due to the switch was measured at various frequencies across the band and are as shown in Table 5.

Discussion of Results:

The theoretical noise contribution ΔT_S of the switch can be calculated from equation (3). Inserting the measured value of switch loss, 0.75 dB, and an assumed physical temperature of 18°K (temperature at which refrigerator was operating) into equation (3) gives a $\Delta T_S = 7.8^\circ\text{K}$. However, the average measured value of ΔT_S is 14.1°K (average of values given in Table 5) and is 6.3°K greater than that calculated by equation (3). This discrepancy can be attributed to three known sources of error: (1) impedance mismatch, (2) shot noise, and (3) uncertainty in the value of physical temperature used in equation (2). The temperature could be significantly higher than 18°K due to diode junction heating caused by the bias current.

The first source of error, impedance mismatch, could account for 0.7°K of the 6.3°K discrepancy. This comes about due to the termination on the par-amp input circulator which can be considered an 18°K noise source. Assuming

the switch has a VSWR of 1.5:1, as measured, 0.7°K of the 18°K can be reflected at the switch and returned to the paramp as an increase in noise temperature.

The remaining 5.6°K of noise can be attributed to short noise and inaccuracy in the known physical temperature T_p ; however, an analysis to determine the magnitude of these two sources of error has not been made.